Journal of Sound and Vibration 329 (2010) 1177–1190

Contents lists available at ScienceDirect

Journal of Sound and Vibration

journal homepage: www.elsevier.com/locate/jsvi

Mode shape expansion using perturbed force approach

Hua-Peng Chen *

School of Engineering, University of Greenwich, Chatham Maritime, Kent ME4 4TB, UK

ARTICLE INFO

Article history:
Received 7 July 2009
Received in revised form
21 October 2009
Accepted 21 October 2009
Handling Editor: C. Morfey
Available online 25 November 2009

ABSTRACT

A new approach for expanding incomplete experimental mode shapes is presented which considers the modelling errors in the analytical model and the uncertainties in the vibration modal data measurements. The proposed approach adopts the perturbed force vector that includes the effect of the discrepancy in mass and stiffness between the finite element model and the actual tested dynamic system. From the developed formulations, the perturbed force vector can be obtained from measured modal data and is then used for predicting the unmeasured components of the expanded experimental mode shapes. A special case that does not require the experimental natural frequency in the mode shape expansion process is also discussed. A regularization algorithm based on the Tikhonov solution incorporating the generalized cross-validation method is employed to filter out the influence of noise in measured modal data on the predictions of unmeasured mode components. The accuracy and robustness of the proposed approach is verified with respect to the size of measured data set, sensor location, model deficiency and measurement uncertainty. The results from two numerical examples, a plane frame structure and a thin plate structure, show that the proposed approach has the best performance compared with the commonly used existing expansion methods, and can reliably produce the predictions of mode shape expansion, even in the cases with limited modal data measurements, large modelling errors and severe measurement noise.

1. Introduction

Mode shape expansion has many applications, such as for test-analysis correlation study, for updating finite element models and for identifying damage in structures [1–4]. In general, the analytical mode shapes obtained from finite element analysis contain a full set of degrees of freedom (DOF) from the analytical model. The measured data set of a dynamic test, however, is usually incomplete and only exists at the DOFs associated with the test points, because the measurements are often taken at a limited set of locations in selected coordinate directions [5,6]. In addition, difficulties in measuring vibration modal data often arise in the cases associated with internal nodes and rotational DOFs. In many structural dynamics applications such as vibration-based model updating and damage identification [7–9], it is desirable to expand the reduced experimental data set onto the associated full finite element coordinate set. The alternative would be a model reduction process which destroys the original sparse pattern in mass and stiffness matrices and propagates modelling errors or structural damage all over the reduced mass and/or stiffness matrices.

Most mode shape expansion methods utilized today involve the use of the model reduction transformation matrix as an expansion mechanism to obtain the unmeasured mode components of the actual tested dynamic system. For example, the

* Tel.: +44 1634 883031; fax: +44 1634 883153.
E-mail addresses: h.chen@greenwich.ac.uk, hp.chen@virgin.net.

0022-460X/$ - see front matter © 2009 Elsevier Ltd. All rights reserved.
doi:10.1016/j.jsv.2009.10.027

Guyan static expansion method [10] is based on the assumption that the inertial forces acting on the unmeasured DOFs can be ignored in the expansion process to provide a simple static transformation matrix for mode shape expansion. The Guyan static method may give accurate mode shape expansion estimates only when there are sufficient DOFs to represent the mass inertia of the actual tested dynamic system. The IRS expansion method, proposed by O'Callahan [11] and later extended by Friswell et al. [12], modifies the Guyan static condensation transformation matrix by adding a term to make some allowance for the ignored mass inertia associated with the unmeasured DOFs. The Kidder dynamic method [13] is similar to the Guyan static method except that the inertial forces at the unmeasured DOFs are considered at a particular frequency. The System Equivalent Reduction Expansion Process (SEREP) method [14] utilizes the analytical mode shapes to generate a transformation matrix between the measured DOFs and the unmeasured DOFs. The SEREP method could produce poor expansion estimates if the experimental mode shapes are not correlated well with the corresponding analytical mode shapes, which often happens in the cases with large modelling errors in the analytical model. In addition, the penalty method [15] uses a weighting variable as a measure of the relative confidence in the experimental mode shapes to produce mode expansion estimates by minimizing the modal strain energy. These existing expansion methods need information about the modal data (frequency and mode shape) or structural parameters (mass and stiffness) of the analytical model in mode shape expansion processes, but they do not consider the modelling errors due to the discrepancy in structural parameters between the analytical model and the actual tested dynamic system. Also, these existing methods do not include effective measures to filter out the influence of inevitable measurement uncertainties on the predictions of mode shape expansion.

This study presents a new approach for expanding mode shapes by introducing a perturbed force vector and utilizing a regularization algorithm in order to include the modelling errors in the analytical model and reduce the influence of noise in measured modal data. The proposed approach takes the perturbed force vector containing modelling errors as basic parameters, which can be obtained from modal data measurements, and then applies it to predicting the unmeasured part of the expanded mode shapes. In order to give stable solutions for the perturbed force vector from the noisy measurements, a regularization algorithm based on the Tikhonov solution incorporating the generalized cross-validation (GCV) method is employed to reduce the effect of measurement noise. An investigation with respect to several evaluation criteria is conducted to compare the proposed approach with the commonly used existing expansion methods and assess the robustness and reliability of the proposed approach. The results from two numerical examples show that the proposed approach dealing with both modelling errors and measurement uncertainties produces by far the most accurate and reliable mode shape expansion results, in particular in severe adverse situations.

2. General expansion methods

For a dynamic structural system with global stiffness matrix $\mathbf{K}$ and mass matrix $\mathbf{M}$, the characteristic equation of an n DOFs dynamic system can be expressed as

$$(\mathbf{K}-\omega_i^2\mathbf{M})\boldsymbol{\phi}_i=\mathbf{0} \tag{1}$$

where ω_i and $\boldsymbol{\phi}_i$ are the ith natural frequency and the corresponding mode shape, respectively. In general, the mode shapes obtained from experiments only exist at the DOFs associated with test points and need to be expanded over the full set of analytical DOFs for structural dynamic applications such as correlation studies, model updating and damage identification. The full set of analytical DOFs then can be divided into two complementary sets, the measured DOFs at the test points and the remaining unmeasured DOFs. The characteristic equation in Eq. (1) can be rewritten in a partitioned form as

$$\begin{bmatrix}\mathbf{K}^{aa} & \mathbf{K}^{au}\\ \mathbf{K}^{ua} & \mathbf{K}^{uu}\end{bmatrix}\begin{Bmatrix}\boldsymbol{\phi}_i^a\\ \boldsymbol{\phi}_i^u\end{Bmatrix}-\omega_i^2\begin{bmatrix}\mathbf{M}^{aa} & \mathbf{M}^{au}\\ \mathbf{M}^{ua} & \mathbf{M}^{uu}\end{bmatrix}\begin{Bmatrix}\boldsymbol{\phi}_i^a\\ \boldsymbol{\phi}_i^u\end{Bmatrix}=\begin{Bmatrix}\mathbf{0}\\ \mathbf{0}\end{Bmatrix} \tag{2}$$

where subscripts a and u denote the measured and unmeasured DOFs, respectively. From the second equation of the partitioned set in Eq. (2), the unmeasured part of the mode shape can be obtained from

$$\boldsymbol{\phi}_i^u=-[\mathbf{K}^{uu}-\omega_i^2\mathbf{M}^{uu}]^{-1}[\mathbf{K}^{ua}-\omega_i^2\mathbf{M}^{ua}]\boldsymbol{\phi}_i^a \tag{3}$$

Consequently, the ith expanded mode shape with full set of DOFs, comprising the measured part $\boldsymbol{\phi}_i^a$ and unmeasured part $\boldsymbol{\phi}_i^u$, is expressed as

$$\boldsymbol{\phi}_i=\begin{Bmatrix}\boldsymbol{\phi}_i^a\\ \boldsymbol{\phi}_i^u\end{Bmatrix}=\mathbf{T}\boldsymbol{\phi}_i^a \tag{4}$$

where $\mathbf{T}$ is the transformation matrix between the reduced set of measured DOFs and the full set of DOFs, depending on the expansion methods adopted.

The static expansion method [10] is based on the static stiffness by neglecting the inertial forces at the unmeasured DOFs. The static transformation matrix $\mathbf{T}_s$ is given by

$$\mathbf{T}_s=\begin{bmatrix}\mathbf{I}\\ -\mathbf{K}^{uu^{-1}}\mathbf{K}^{ua}\end{bmatrix} \tag{5}$$

The dynamic expansion method [13] is the same as the static expansion method except that the inertial forces at the unmeasured DOFs are included in the expansion process. From Eq. (3), the dynamic transformation matrix $\mathbf{T}_d$ is given by

$$\mathbf{T}_d = \begin{bmatrix} \mathbf{I} \\ -[\mathbf{K}^{uu} - \omega_i^2 \mathbf{M}^{uu}]^{-1}[\mathbf{K}^{ua} - \omega_i^2 \mathbf{M}^{ua}] \end{bmatrix} \tag{6}$$

The SEREP expansion method [14] is not directly related to the stiffness and mass of the analytical model and depends on analytical mode shapes to develop the mapping between the full set of analytical DOFs and the reduced set of measured DOFs. In the case when the number of measured DOFs is greater than the number of modes in the tested structure, the SEREP transformation matrix $\mathbf{T}_u$ is expressed as

$$\mathbf{T}_u = \begin{Bmatrix} \boldsymbol{\phi}^a \\ \boldsymbol{\phi}^u \end{Bmatrix} [\boldsymbol{\phi}^{a^{\mathrm{T}}} \ \boldsymbol{\phi}^a]^{-1} \boldsymbol{\phi}^{a^{\mathrm{T}}} \tag{7}$$

where superscript T denotes the transpose of a vector or matrix quantity throughout this paper. In the SEREP expansion process, the initial displacements at the measured DOF's may be modified.

The existing methods discussed above are often used to expand the measured incomplete mode shapes in structural dynamic applications. However, these methods do not consider the discrepancy between the analytical model and the actual tested structure, since only the structural or modal parameters associated with the analytical model are utilized in the mode expansion processes. In addition, the displacements at the measured DOF's are directly adopted for mode shape expansion and the influence of measurement uncertainty cannot be reduced.

3. Perturbed force approach

3.1. Model uncertainty and perturbed force

In structural dynamic applications, the finite element model usually has uncertainties in modelling the associated actual tested structural dynamic system. The model uncertainties are mainly related to the unknown perturbations of stiffness ($\Delta\mathbf{K}$) and mass ($\Delta\mathbf{M}$) between the analytical model and the tested system. The global stiffness matrix ($\tilde{\mathbf{K}}$) and mass matrix ($\tilde{\mathbf{M}}$) of the tested dynamic structure then can be expressed as

$$\tilde{\mathbf{K}} = \mathbf{K} + \Delta\mathbf{K} \tag{8a}$$

$$\tilde{\mathbf{M}} = \mathbf{M} + \Delta\mathbf{M} \tag{8b}$$

The characteristic equation for the experimental structural dynamic system is given by

$$(\tilde{\mathbf{K}} - \tilde{\omega}_i^2 \tilde{\mathbf{M}})\tilde{\boldsymbol{\phi}}_i = 0 \tag{9}$$

where $\tilde{\omega}_i$ and $\tilde{\boldsymbol{\phi}}_i$ are the ith natural frequency and the corresponding mode shape for the tested system, respectively. Substituting Eqs. (8a) and (8b) into the experimental characteristic equation in Eq. (9), gives

$$[(\Delta\mathbf{K} - \tilde{\omega}_i^2 \Delta\mathbf{M}) + (\mathbf{K} - \tilde{\omega}_i^2 \mathbf{M})]\tilde{\boldsymbol{\phi}}_i = 0 \tag{10}$$

Pre-multiplying Eq. (10) by $\boldsymbol{\phi}_k^{\mathrm{T}}$ and using the transpose of the characteristic equation for the analytical model shown in Eq. (1), leads to

$$\boldsymbol{\phi}_k^{\mathrm{T}}(\Delta\mathbf{K} - \tilde{\omega}_i^2 \Delta\mathbf{M})\tilde{\boldsymbol{\phi}}_i - (\tilde{\omega}_i^2 - \omega_k^2)\boldsymbol{\phi}_k^{\mathrm{T}}\mathbf{M}\tilde{\boldsymbol{\phi}}_i = 0 \tag{11}$$

Define a perturbed force vector for the ith mode, associated with the unknown perturbations of stiffness and mass, as

$$\mathbf{r}_i = (\Delta\mathbf{K} - \tilde{\omega}_i^2 \Delta\mathbf{M})\tilde{\boldsymbol{\phi}}_i \tag{12}$$

The perturbed force vector $\mathbf{r}_i$ in Eq. (12) becomes zero if both $\Delta\mathbf{K}$ and $\Delta\mathbf{M}$ are equal to zero, i.e. no structural modelling errors exist in the analytical mode. Eq. (11), by using the introduced perturbed force vector, can be rewritten as

$$\boldsymbol{\phi}_k^{\mathrm{T}}\mathbf{M}\tilde{\boldsymbol{\phi}}_i = \frac{\boldsymbol{\phi}_k^{\mathrm{T}}\mathbf{r}_i}{(\tilde{\omega}_i^2 - \omega_k^2)} \tag{13}$$

Notice that the eigenvectors of the analytical model $\boldsymbol{\phi}_i$ are linearly independent since its stiffness and mass matrices are symmetric. The mode shapes of the tested structure then can be expressed as a linear combination of the independent analytical eigenvectors

$$\tilde{\boldsymbol{\phi}}_i = \sum_{k=1}^{n} C_{ik}\boldsymbol{\phi}_k \tag{14}$$

where C_{ik} are mode participation factors. It is assumed here that the analytical eigenvectors are normalized as unity with respect to the mass. Premultiplying Eq. (14) by $\boldsymbol{\phi}_k^{\mathrm{T}}\mathbf{M}$, and using the mass normalization of the analytical

eigenvectors, yields

$$C_{ik} = \boldsymbol{\phi}_k^{\mathrm{T}} \mathbf{M} \tilde{\boldsymbol{\phi}}_i \tag{15}$$

From Eq. (13), the mode participation factors C_{ik} in Eq. (15) are rewritten as

$$C_{ik} = \frac{\boldsymbol{\phi}_k^{\mathrm{T}} \mathbf{r}_i}{(\tilde{\omega}_i^2 - \omega_k^2)} \tag{16}$$

Substituting the mode participation factors in Eq. (16) into Eq. (14), yields

$$\sum_{k=1}^{n} \frac{\boldsymbol{\phi}_k^{\mathrm{T}} \mathbf{r}_i}{(\tilde{\omega}_i^2 - \omega_k^2)} \boldsymbol{\phi}_k = \tilde{\boldsymbol{\phi}}_i \tag{17}$$

3.2. General transformation matrix

n structural dynamic testing for the experimental structure, modal information about natural frequency $\tilde{\omega}_i$ and limited number of measured DOF's $\tilde{\boldsymbol{\psi}}_i$ of dimension m can be obtained. The incomplete set of measured DOF's $\tilde{\boldsymbol{\psi}}_i$ need to be scaled with a factor in order to make the measured mode shapes close to the corresponding part of the analytical mode shapes $\boldsymbol{\phi}_i^a$, as

$$\tilde{\boldsymbol{\phi}}_i^{\,a} = \beta_i \tilde{\boldsymbol{\psi}}_i \tag{18}$$

in which mode scale factor β_i is defined as

$$\beta_i = \frac{\boldsymbol{\phi}_i^{a^{\mathrm{T}}} \tilde{\boldsymbol{\psi}}_i}{\tilde{\boldsymbol{\psi}}_i^{\mathrm{T}} \tilde{\boldsymbol{\psi}}_i} \tag{19}$$

Considering only measured DOF's in Eq. (17) for the mode shapes of the tested system, Eq. (17) is now rewritten in a matrix format

$$\mathbf{S}_i \mathbf{r}_i = \tilde{\boldsymbol{\phi}}_i^{\,a} \tag{20}$$

where sensitivity coefficient matrix of dimension $m \times n$ for the ith experimental mode $\mathbf{S}_i$, which is related to the analytical mode shapes corresponding to the measured components $\boldsymbol{\phi}_k^a$, is defined as

$$\mathbf{S}_i = \sum_{k=1}^{NC} \frac{\boldsymbol{\phi}_k^a \boldsymbol{\phi}_k^{\mathrm{T}}}{(\tilde{\omega}_i^2 - \omega_k^2)} \tag{21}$$

in which NC denotes the number of the original eigenvectors available, and is used here to replace the total number of DOFs n in Eq. (17), since the terms with subscripts greater than k can be neglected, when k is large enough. The perturbed force vector for the ith experimental mode then can be directly calculated from

$$\mathbf{r}_i = \mathbf{S}_i^{+} \tilde{\boldsymbol{\phi}}_i^{\,a} \tag{22}$$

where $\mathbf{S}_i^{+}$ is the Moore–Penrose pseudoinverse of matrix $\mathbf{S}_i$, given by

$$\mathbf{S}_i^{+} = \mathbf{S}_i^{\mathrm{T}} [\mathbf{S}_i \mathbf{S}_i^{\mathrm{T}}]^{-1} \tag{23}$$

By using Eq. (22), the mode participation factors in Eq. (16) are now written as

$$C_{ik} = \frac{\boldsymbol{\phi}_k^{\mathrm{T}} \mathbf{S}_i^{+} \tilde{\boldsymbol{\phi}}_i^{\,a}}{(\tilde{\omega}_i^2 - \omega_k^2)} \tag{24}$$

The unmeasured part of the ith mode shape of the tested system can be calculated from Eq. (14) where the mode participation factors C_{ik} are given in Eq. (24), namely

$$\tilde{\boldsymbol{\phi}}_i^{\,u} = \sum_{k=1}^{NC} \frac{\boldsymbol{\phi}_k^u \boldsymbol{\phi}_k^{\mathrm{T}} \mathbf{S}_i^{+}}{(\tilde{\omega}_i^2 - \omega_k^2)} \tilde{\boldsymbol{\phi}}_i^{\,a} \tag{25}$$

Consequently, the ith full experimental mode shape, consisting the measured part $\tilde{\boldsymbol{\phi}}_i^{\,a}$ and the unmeasured part $\tilde{\boldsymbol{\phi}}_i^{\,u}$, can be obtained from

$$\tilde{\boldsymbol{\phi}}_i = \begin{Bmatrix} \tilde{\boldsymbol{\phi}}_i^{\,a} \\ \tilde{\boldsymbol{\phi}}_i^{\,u} \end{Bmatrix} = T_p^i \tilde{\boldsymbol{\phi}}_i^{\,a} \tag{26}$$

where the transformation matrix $\mathbf{T}_p^i$ of the proposed approach is defined as

$$\mathbf{T}_p^i = \begin{bmatrix} \mathbf{I} \\ \sum_{k=1}^{NC} \dfrac{\boldsymbol{\phi}_k^u \boldsymbol{\phi}_k^{\mathrm{T}} \mathbf{S}_i^+}{(\tilde{\omega}_i^2 - \omega_k^2)} \end{bmatrix} \tag{27}$$

It is found that the proposed transformation matrix depends on the individual experimental mode to be expanded since it includes the associated experimental natural frequency $\tilde{\omega}_i$. The experimental frequency $\tilde{\omega}_i$ is assumed to be different from ω_k where k=1, NC, or the following formulation for the special case should be utilized.

3.3. Expansion for special case

In the special case when the experimental frequency is not available or equals one of the analytical frequencies, it is necessary to modify the transformation matrix in Eq. (27). Rearranging Eq. (11) and using Eq. (8b), leads to

$$\boldsymbol{\phi}_k^{\mathrm{T}}(\Delta\mathbf{K} - \tilde{\omega}_i^2 \tilde{\mathbf{M}})\tilde{\boldsymbol{\phi}}_i + \omega_k^2 \boldsymbol{\phi}_k^{\mathrm{T}} \mathbf{M} \tilde{\boldsymbol{\phi}}_i = 0 \tag{28}$$

Redefine a perturbed force vector for the ith mode, which is the same as the definition in Eq. (12) except that the mass of the tested structure is used here to replace the perturbation of the mass, as

$$\mathbf{r}_i' = (\Delta\mathbf{K} - \tilde{\omega}_i^2 \tilde{\mathbf{M}})\tilde{\boldsymbol{\phi}}_i \tag{29}$$

Similarly, the mode participation factors for the special case are then given by

$$C_{ik}' = \boldsymbol{\phi}_k^{\mathrm{T}} \mathbf{M} \tilde{\boldsymbol{\phi}}_i = -\frac{\boldsymbol{\phi}_k^{\mathrm{T}} \mathbf{r}_i'}{\omega_k^2} \tag{30}$$

The perturbed force vector for the special case $\mathbf{r}_i'$ then can be calculated from

$$\mathbf{S}_i' \mathbf{r}_i' = \tilde{\boldsymbol{\phi}}_i^a \tag{31}$$

where the sensitivity coefficient matrix for the special case $\mathbf{S}_i'$ is defined as

$$\mathbf{S}_i' = \sum_{k=1}^{NC} -\frac{\boldsymbol{\phi}_k^a \boldsymbol{\phi}_k^{\mathrm{T}}}{\omega_k^2} \tag{32}$$

Consequently, the transformation matrix for the special case $\mathbf{T}_p'^i$, by solving Eq. (31) and using the Moore–Penrose pseudoinverse for the special case $\mathbf{S}_i'^+$, can be expressed as

$$\mathbf{T}_p'^i = \begin{bmatrix} \mathbf{I} \\ -\sum_{k=1}^{NC} \dfrac{\boldsymbol{\phi}_k^u \boldsymbol{\phi}_k^{\mathrm{T}} \mathbf{S}_i'^+}{\omega_k^2} \end{bmatrix} \tag{33}$$

It is found that the transformation matrix of the proposed approach is only related to the modal data of the analytical model and no knowledge of the mass and stiffness of the analytical model is needed in the calculations. The proposed approach successfully includes the effect of structural modelling errors in the analytical model due to the perturbation of mass and stiffness by introducing the perturbed force vector. However, it is not necessary to quantify the structural modelling errors in the analytical model.

4. Expansion to include regularization method

Due to the inevitable noise in modal data measurements, the solution of the perturbed force vector obtained from the Moore–Penrose pseudoinverse in Eq. (22) may not be stable. In order to reduce the influence of noise in modal data measurements on the performance of mode shape expansion, a regularization method is now employed to obtain reasonable solutions for the perturbed force vector. Consider the linear system in Eq. (20) for solving the perturbed force vector $\mathbf{r}_i$ (the same process can be applied to the special case given in Eq. (31)), rewritten here as

$$\mathbf{S}_{i(m\times n)} \mathbf{r}_{i(n\times 1)} = \tilde{\boldsymbol{\phi}}_{i(m\times 1)}^a \tag{34}$$

where m represents the total number of measured noisy DOF's readings of the tested system and is not greater than the total number of DOFs, i.e. $m \leq n$. It should be noted that the sensitivity coefficient matrix $\mathbf{S}_i$ is only related to the analytical modal data and experimental frequency and can be estimated at a relatively high level of accuracy. Let the singular value decomposition (SVD) of the sensitivity coefficient matrix $\mathbf{S}_i$ be

$$\mathbf{S}_{i(m\times n)} = \mathbf{U}_{(m\times m)} \boldsymbol{\Sigma}_{(m\times n)} \mathbf{V}_{(n\times n)}^{\mathrm{T}} = \sum_{j=1}^{m} \sigma_j \mathbf{u}_j \mathbf{v}_j^{\mathrm{T}} \tag{35}$$

where $\mathbf{\Sigma}$ is a diagonal matrix containing strictly non-negative and non-increasing singular values σ_j. The orthonormal column vectors $\mathbf{u}_j$ of $\mathbf{U}$ and $\mathbf{v}_j$ of $\mathbf{V}$ are the left and right singular vectors, respectively, corresponding to σ_j. It can be shown that the ordinary least squares solution to Eq. (34) can be expressed as

$$\mathbf{r}_i = \sum_{j=1}^{m} \frac{\mathbf{u}_j^{\mathrm{T}} \tilde{\boldsymbol{\phi}}_i^a}{\sigma_j} \mathbf{v}_j \tag{36}$$

In order to obtain stable and reliable solutions for the perturbed force vector, some sort of regularization of the problem is required to filter out the contributions of the noise contained in $\tilde{\boldsymbol{\phi}}_i^a$. One of the most commonly used regularization methods with a continuous regularization parameter is the Tikhonov regularization [16]. The regularization replaces the original operation with a better-conditioned but related one and produces a regularized solution to the original problem. The Tikhonov regularized solution for a continuous regularization parameter α, replacing the direct solution in Eq. (22), is given in terms of the SVD in Eq. (35) as

$$\mathbf{r}_i(\alpha) = \mathbf{S}_i^{\#}(\alpha) \tilde{\boldsymbol{\phi}}_i^a \tag{37}$$

where $\mathbf{S}_i^{\#}(\alpha)$ is the influence matrix, associated with the Tikhonov regularization parameter α, defined as

$$\mathbf{S}_i^{\#}(\alpha) = \sum_{j=1}^{m} \frac{f_j(\alpha)}{\sigma_j} \mathbf{v}_j \mathbf{u}_j^{\mathrm{T}} \tag{38}$$

in which $f_j(\alpha)$ are the Tikhonov filter factors, depending on singular values σ_j and regularization parameter α, defined as

$$f_j(\alpha) = \frac{\sigma_j^2}{\sigma_j^2 + \alpha^2} \approx \begin{cases} 1 & \text{if } \sigma_j \gg \alpha \\ \dfrac{\sigma_j^2}{\alpha^2} & \text{if } \sigma_j \ll \alpha \end{cases} \tag{39}$$

A stable solution then can be obtained since the Tikhonov regularized solution coefficients $f_j(\alpha)|\mathbf{u}_j^{\mathrm{T}} \tilde{\boldsymbol{\phi}}_i^a|/\sigma_j$ are gradually attenuated as singular values decrease. The filter factors $f_j(\alpha)$ increasingly filter out the contributions to $\mathbf{r}_i(\alpha)$ associated with the small singular values, whereas the contributions associated with the large singular values are almost unaffected. The Tikhonov regularization parameter α has to be chosen according to the random noise level in modal data measurements. In reality, the noise level for the measured modal data is often unknown. Thus, the generalized cross-validation (GCV) method [17] is employed to estimate the optimal value of the Tikhonov regularization parameter α, because this method does not require a priori information about the noise level. The GCV function used to estimate the Tikhonov regularization parameter α is defined as

$$G(\alpha) = \frac{\frac{1}{m} \| [\mathbf{I} - \mathbf{S}_i \mathbf{S}_i^{\#}(\alpha)] \tilde{\boldsymbol{\phi}}_i^a \|_2^2}{\left\{ \frac{1}{m} \mathrm{Trace}[\mathbf{I} - \mathbf{S}_i \mathbf{S}_i^{\#}(\alpha)] \right\}^2} \tag{40}$$

where $\mathbf{I}$ is the identity matrix and the optimum value of α is found where G is minimized. Considering the SVD of the sensitivity coefficient matrix $\mathbf{S}_i$ in Eq. (35) and the regularized SVD solution $\mathbf{r}_i(\alpha)$ in Eq. (37), the residual norm in the numerator and the trace in the denominator of the GCV function can be computed from

$$\| [\mathbf{I} - \mathbf{S}_i \mathbf{S}_i^{\#}(\alpha)] \tilde{\boldsymbol{\phi}}_i^a \|_2^2 = \| \tilde{\boldsymbol{\phi}}_i^a - \mathbf{S}_i \mathbf{r}_i(\alpha) \|_2^2 = \sum_{i=1}^{m} [(1 - f_i(\alpha)) \mathbf{u}_i^{\mathrm{T}} \tilde{\boldsymbol{\phi}}_i^a]^2 \tag{41.a}$$

$$\mathrm{Trace}[\mathbf{I} - \mathbf{S}_i \mathbf{S}_i^{\#}(\alpha)] = \sum_{i=1}^{m} (1 - f_i(\alpha)) \tag{41.b}$$

The GCV function in Eq. (40) then can be rewritten as

$$G(\alpha) = \frac{m \sum_{i=1}^{m} [(1 - f_i(\alpha)) \mathbf{u}_i^{\mathrm{T}} \tilde{\boldsymbol{\phi}}_i^a]^2}{[\sum_{i=1}^{m} (1 - f_i(\alpha))]^2} \tag{42}$$

For the case with errors in modal data measurements, there exists an optimum Tikhonov regularization parameter α^* such that the GCV function given in Eq. (42) reaches its minimum, as indicated in the example discussed in Section 6.

5. Evaluation of expanded mode shape

In order to assess the performance of the proposed approach, it is assumed that the full set of actual mode shapes of the tested structure $\tilde{\boldsymbol{\phi}}_i^*$ as well as its mass $\tilde{\mathbf{M}}$ and stiffness $\tilde{\mathbf{K}}$ are available. These are purely used here as a reference for performance evaluation. Several evaluation criteria are introduced to compare the proposed approach with the existing expansion methods and assess the mode shape expansion predictions by the proposed approach. The Modal Assurance Criterion (MAC) factors are used here to verify the correlation between the expanded experimental mode shapes and the

corresponding analytical mode shapes [5], defined as

$$\mathrm{MAC}(k,i)=\frac{|\boldsymbol{\phi}_k^{\mathrm{T}}\tilde{\boldsymbol{\phi}}_i|^2}{|\boldsymbol{\phi}_k^{\mathrm{T}}\boldsymbol{\phi}_k||\tilde{\boldsymbol{\phi}}_i^{\mathrm{T}}\tilde{\boldsymbol{\phi}}_i|} \tag{43}$$

From the definition, large MAC factors indicate a high degree of similarity between two mode shapes and small MAC factors represent little or even no correlation between two vectors.

In order to evaluate the errors at each DOF between the predicted experimental mode shape $\tilde{\boldsymbol{\phi}}_i$ and the ideal actual mode shape $\tilde{\boldsymbol{\phi}}_i^*$, a relative mode error for the ith mode with respect to the mass of the tested structure $\tilde{\mathbf{M}}$ is defined as

$$e_P^i=\frac{(\tilde{\boldsymbol{\phi}}_i-\tilde{\boldsymbol{\phi}}_i^*)^{\mathrm{T}}\tilde{\mathbf{M}}(\tilde{\boldsymbol{\phi}}_i-\tilde{\boldsymbol{\phi}}_i^*)}{\tilde{\boldsymbol{\phi}}_i^{*\mathrm{T}}\tilde{\mathbf{M}}\tilde{\boldsymbol{\phi}}_i^*} \tag{44}$$

The relative mode error becomes zero if the expanded experimental mode shape is ideally predicted. The mean cumulative error is then introduced to evaluate the overall performance for a total number of NM expanded modes, defined as

$$E_P=\frac{1}{NM}\sum_{i=1}^{NM}e_P^i \tag{45}$$

The orthogonality performance criteria are adopted to measure the cross orthogonality of the predicted mode shapes with respect to the actual mass and stiffness. The average mass and stiffness orthogonality errors are defined as, respectively,

$$E_M=\frac{1}{\frac{1}{2}NM(NM-1)}\sum_{i=1}^{NM}\sum_{j=i+1}^{NM}\left(\frac{\tilde{m}_{ij}^2}{\tilde{m}_{ii}\tilde{m}_{jj}}\right)^{1/2} \tag{46a}$$

$$E_K=\frac{1}{\frac{1}{2}NM(NM-1)}\sum_{i=1}^{NM}\sum_{j=i+1}^{NM}\left(\frac{\tilde{k}_{ij}^2}{\tilde{k}_{ii}\tilde{k}_{jj}}\right)^{1/2} \tag{46b}$$

where coefficients $\tilde{m}_{ij}$ and $\tilde{k}_{ij}$ are calculated from

$$\tilde{m}_{ij}=\tilde{\boldsymbol{\phi}}_i^{\mathrm{T}}\tilde{\mathbf{M}}\tilde{\boldsymbol{\phi}}_j \tag{47a}$$

$$\tilde{k}_{ij}=\tilde{\boldsymbol{\phi}}_i^{\mathrm{T}}\tilde{\mathbf{K}}\tilde{\boldsymbol{\phi}}_j \tag{47b}$$

By using the perturbations of stiffness ($\Delta\mathbf{K}$) and mass ($\Delta\mathbf{M}$) between the analytical model and the tested system given in Eq. (8) and considering the mode shapes of the tested structure $\tilde{\boldsymbol{\phi}}_i$ expressed as a function of the mode participation factors C_{ik} given in Eq. (14), the coefficients $\tilde{m}_{ij}$ and $\tilde{k}_{ij}$ can be further expressed as

$$\tilde{m}_{ij}=\sum_{k=1}^{NC}C_{ik}C_{jk}+\sum_{k=1}^{NC}\sum_{l=1}^{NC}C_{ik}C_{jl}\boldsymbol{\phi}_k^{\mathrm{T}}\Delta\mathbf{M}\boldsymbol{\phi}_l \tag{48a}$$

$$\tilde{k}_{ij}=\omega_j^2\sum_{k=1}^{NC}C_{ik}C_{jk}+\sum_{k=1}^{NC}\sum_{l=1}^{NC}C_{ik}C_{jl}\boldsymbol{\phi}_k^{\mathrm{T}}\Delta\mathbf{K}\boldsymbol{\phi}_l \tag{48b}$$

The overall orthogonality error with respect to both mass and stiffness can then be defined as

$$E_{MK}=(E_M^2+E_K^2)^{1/2} \tag{49}$$

In these formulations, the orthogonality errors are small if the expanded mode shapes are well predicted. The mass and stiffness cross orthogonality is completely satisfied if the expanded mode shapes are the same as the corresponding ideal actual mode shapes.

6. Numerical example

Two numerical examples, a plane frame model and a thin plate model, are employed to demonstrate the accuracy and effectiveness of the proposed mode shape expansion technique. The results obtained from the proposed approach for the two different types of structure models are then compared with those from commonly used existing expansion methods outlined in Section 2 with respect to the performance evaluation criteria defined in the preceding section. Several simulated scenarios are considered to assess the robustness and reliability of the proposed approach, such as the size and location of sensors, modelling errors in the analytical model and added noise in modal data measurements.

6.1. Plane frame structure

The first structure used to demonstrate the proposed approach is the plane frame structure model shown in Fig. 1. A finite element model for the structure is developed by utilizing the direct stiffness method with three DOFs at each node, two translational displacements and one rotational displacement. The developed analytical model has a total number of 28 conventional beam elements with axial deformations and a total number of 81 DOFs. The plane frame model structure has section properties of area A=9.20 × 10^{-3} m^2 and moment of inertia I=4.52 × 10^{-6} m^4 and material properties of Young's modulus E=7.20 × 10^{10} N/m^2 and density ρ=2700 kg/m^3. It is assumed that the actual tested frame structure has perturbations of stiffness of +15 percent and mass of −10 percent at elements 1–16 for the columns and additional perturbations of stiffness of −10 percent and mass of +10 percent at elements 17–28 for the beams. The incomplete mode shapes of the tested structure are assumed to be obtained from the possible sensor locations measuring only translational DOF's, as indicated in Fig. 1.

A finite element analysis was performed for both the analytical model and the tested structure to calculate natural frequencies and the corresponding mode shapes. In the following, the computed frequencies and the corresponding measured DOF's of the actual tested structure are adopted in calculations in place of the measured experimental modal data, which would normally be furnished from experiments. The first ten modes of the analytical model and the assumed actual structure are listed in Table 1. It is found that there exists considerable difference ranging from −4.54 to 5.93 percent in frequency between the analytical model and the actual tested structure due to the relatively large perturbations of mass and stiffness. The lower modes 1–7 of the analytical model and tested structure are well correlated with MAC diagonal values close to unity.

The results in Table 2 show the evaluation of expanded mode shapes predicted by the existing methods and the proposed approach. Here, only four sensors at beam–column joints of the frame structure with a total number of eight DOF's readings are utilized as the measured set and expanded to full 81 DOFs described in the analytical model. The proposed approach is then compared with the existing methods, i.e. the static in Eq. (5), dynamic in Eq. (6) and SEREP in Eq. (7). The static method expands only the first mode properly with an MAC value close to ideal value. The expanded modes 2–10 are not represented at all with large relative mode errors and little or no correlation with the corresponding analytical modes. The dynamic method is capable of producing the expansion estimates of modes 1–3 with reasonable relative mode errors, but there are significant relative mode errors in the expanded modes 4–10. The SEREP method generates mode shape expansion estimates that are similar to the dynamic expansion in this case. The proposed approach performs much better across all expanded modes with a mean cumulative error of 6.71 percent, and the predicted MAC diagonal values are consistent with the ideal values given in Table 1. The proposed approach gives more accurate mode shape estimates for modes 1–7 and also produces well the orthogonality with respect to mass and stiffness.

In order to investigate the influence of the number of measured DOF's on the performance of mode shape expansion, ten sensors at beam–column joints and the middle of beams and columns with a total number of 20 DOF's readings are now adopted in predicting mode shape expansion, as shown in Table 3. As expected, the performance of the proposed approach

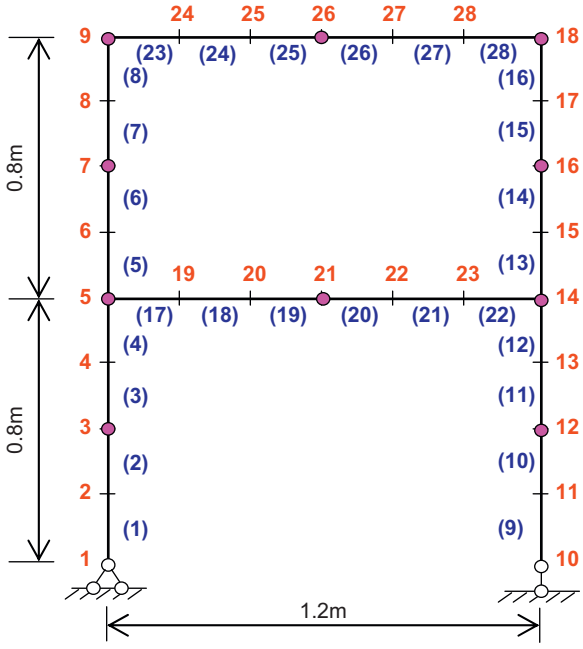

Fig. 1. Plane frame model problem with possible sensor locations marked with '•'.

Table 1
Ideal modes for analytical model and assumed actual plane frame structure.

Mode	Analytical frequency (Hz)	Actual frequency (Hz)	Difference in frequency (%)	MAC diagonal value
1	14.2581	14.7500	3.45	0.9989
2	60.9459	63.3328	3.92	0.9960
3	113.8582	119.6522	5.09	0.9944
4	179.4797	174.0416	−3.03	0.9907
5	217.2696	207.4137	−4.54	0.9893
6	361.0807	382.4889	5.93	0.9797
7	447.2596	467.3444	4.49	0.9523
8	495.1089	510.1664	3.04	0.5366
9	531.4635	551.1520	3.70	0.6709
10	645.2823	682.6392	5.79	0.8722

Table 2
Expanded mode shapes from existing methods and proposed approach, using ideal measurements from four sensors at beam–column joints of frame structure.

Mode	Static		Dynamic		SEREP		Proposed	
	Error e_P^i (%)	MAC	Error e_P^i (%)	MAC	Error e_P^i (%)	MAC	Error e_P^i (%)	MAC
1	0.53	0.9983	0.55	0.9995	48.39	0.5243	1.38	0.9992
2	43.85	0.6417	15.09	0.9904	91.38	0.0159	1.91	0.9978
3	93.11	0.0486	16.19	0.9977	57.64	0.3485	3.22	0.9967
4	98.98	0.0016	53.25	0.7367	18.22	0.9302	3.27	0.9936
5	98.86	0.0006	27.40	0.8776	20.17	0.9255	6.93	0.9931
6	101.30	0.0056	65.34	0.8237	94.62	0.0271	6.26	0.9861
7	117.85	0.0252	62.38	0.7564	49.05	0.8874	5.59	0.9562
8	86.94	0.0000	106.95	0.0568	56.42	0.5174	12.27	0.6307
9	86.51	0.0834	59.76	0.8698	54.39	0.4027	14.26	0.6969
10	96.45	0.0070	102.26	0.2686	86.94	0.8299	12.01	0.8683
Error E_P	82.44		50.92		57.72		6.71	
Error E_M	46.64		14.75		20.69		2.30	
Error E_K	20.26		7.13		21.40		3.23	
Error E_{MK}	50.85		16.38		29.77		3.97	

Table 3
Expanded mode shapes from existing methods and proposed approach, using ideal measurements from ten sensors at beam–column joints and middles of beams and columns.

Mode	Static		Dynamic		SEREP		Proposed	
	Error e_P^i (%)	MAC	Error e_P^i (%)	MAC	Error e_P^i (%)	MAC	Error e_P^i (%)	MAC
1	0.12	0.9988	0.10	0.9989	0.26	0.9984	0.16	0.9986
2	3.28	0.9903	1.48	0.9976	1.31	0.9944	0.65	0.9959
3	9.19	0.9852	3.10	0.9924	1.99	0.9950	2.81	0.9945
4	6.15	0.9778	3.68	0.9863	14.40	0.9104	1.03	0.9909
5	8.42	0.9606	9.40	0.9689	27.51	0.8564	1.42	0.9899
6	27.09	0.9311	6.93	0.9897	6.62	0.9893	4.25	0.9848
7	62.88	0.4230	11.71	0.9494	10.28	0.9722	5.03	0.9624
8	68.55	0.7099	17.29	0.5838	14.69	0.6236	6.43	0.5423
9	73.36	0.0036	18.46	0.5445	20.42	0.6655	7.68	0.6582
10	141.63	0.1239	71.08	0.3122	60.76	0.8370	7.46	0.8700
Error E_P	40.07		14.32		15.82		3.69	
Error E_M	17.56		4.67		5.95		1.14	
Error E_K	8.65		3.58		6.26		1.62	
Error E_{MK}	19.57		5.89		8.64		1.98	

as well as the existing methods improves as the number of measured DOF's increases. Again, the proposed approach performs better for the predictions of mode shape expansion, in particular for lower modes 1–5, with smaller mean cumulative error, more satisfied mass and stiffness cross orthogonality and closer correlation with the corresponding analytical modes.

The effectiveness of the proposed technique for mode shape expansion with respect to the number of analytical eigenvectors available is investigated in the case with ten sensors, as shown in Fig. 2. It is found that the proposed approach requires only a limited knowledge of the analytical modes for correctly estimating mode shape expansion, even a total number of 24 analytical modes is sufficient to give good mode shape expansion results. The performance of mode shape expansion improves very slowly after this number.

Noise in the measured modal data is inevitable and can affect the performance of the mode shape expansion. In this study, the noise in modal data measurements is simulated by corrupting the ideal modal data with additive standard normally distributed errors at different levels. It is assumed here that the noisy modal data measurements have a noise level of 1 percent for measured natural frequencies and noise levels ranging from 1 to 10 percent for the measured DOF's readings at the selected ten sensor locations. The results in Fig. 3 show the applications of the Tikhonov regularization incorporating the GCV method to reduce the effect of measurement errors where the case with ten sensors measuring displacements at various noise levels is considered for predicting the expansion of mode 2. The singular values of the sensitivity coefficient matrix range from 2.12×10^{-5} to 2.28×10^{-10} and the ratio between the largest and the smallest singular values is large. The ordinary solution given in Eq. (36) therefore may not be reliable due to the nature of ill-conditioned system and the noise present in measurements. In order to obtain reliable solutions for the perturbed force vector from the proposed regularization algorithm, an optimum regularization parameter could be evaluated by minimizing the GCV function given in Eq. (42), offering a value of, for example, $\alpha^*=3.66\times10^{-7}$ for the case with noise level of 6 percent. From the results shown in Fig. 3, the values of optimum regularization parameters increase as the levels of noise in the displacements at the measured displacements become high. This indicates that more regularization is imposed on the solution and information on the measured data is gradually lost with the increase of noise level.

The results from the existing methods and the proposed approach are summarized in Figs. 4 and 5 where the mean cumulative errors and the overall orthogonality errors for the first ten expanded modes are plotted as a function of simulated noise level. As before, the static method has the overall worst performance, and fails to produce acceptable mode

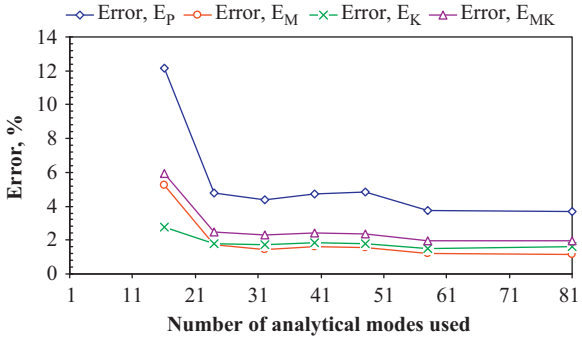

Fig. 2. Influence of the number of analytical modes used on the mode shape expansion predicted by the proposed approach.

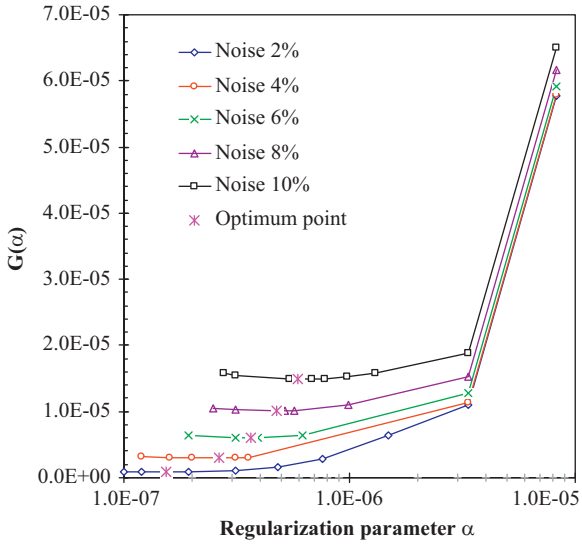

Fig. 3. The GCV function G plotted against the regularization parameter α for cases with various noise levels, giving the optimum regularization parameters.

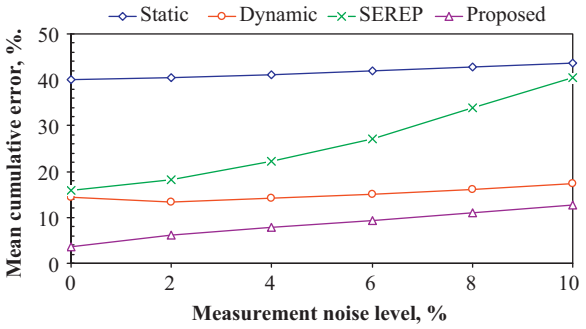

Fig. 4. Mean cumulative errors in mode shape expansion as a function of noise level in DOF's readings for plane frame structure.

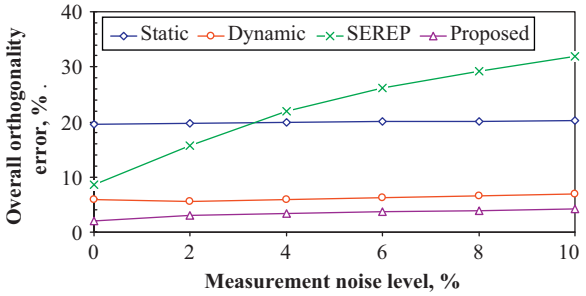

Fig. 5. Overall orthogonality errors in mode shape expansion as a function of noise level in DOF's readings for plane frame structure.

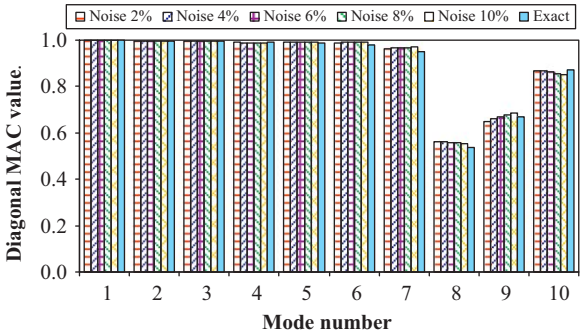

Fig. 6. MAC diagonal values of expanded modes predicted by the proposed approach at various noise levels for plane frame structure.

shape expansion estimates. The SEREP method is the most sensitive to the noise level in measured displacements, generating significant mean cumulative errors and overall orthogonality errors as noise level increases. The dynamic method yields substantial mean cumulative errors and overall orthogonality errors even in the cases with low noise levels. Here again, the proposed approach is capable of expanding mode shapes to a greater level of accuracy than the commonly used existing expansion methods, giving mean cumulative error of 12.8 percent and overall orthogonality error of 4.2 percent, even in the case when the noise level reaches 10 percent. Also, the proposed approach produces well correlated expanded mode shapes with the MAC diagonal values close to the ideal values, as shown in Fig. 6.

6.2. *Thin plate structure*

A rectangular thin plate model shown in Fig. 7 is utilized to demonstrate the performance of the proposed technique for expanding mode shapes from very limited modal data measurements for a continuum structure with a relatively large number of DOFs. The rectangular aluminium plate has dimensions of 1000 mm long, 600 mm wide and 10 mm thick, with material properties of Young's modulus E=6.89 $\times$ 10^{10} N/m^2, Poisson's ratio υ=0.30 and density ρ=2796 kg/m^3. The thin plate is modelled as a plate bending problem with a fixed boundary condition at one of its shorter sides. A finite element model for the thin plate structure is developed by using 8-node isoparametric plate bending elements with three DOFs at each node, i.e. one translational displacement and two rotational displacements. The full analytical model contains 60

elements, 213 nodes and 639 DOFs, and is measured at 15 locations shown in Fig. 7 and marked with ●. It is assumed here that the modelling errors exist over the shaded areas and the thickness of the actual tested plate structure is modified by an increase of 40 percent to a thickness of 14 mm over the shaded areas. Only 15 measured displacements in vertical direction containing up to 10 percent noise are adopted for expanding the incomplete mode shapes. A finite element analysis was performed for both the analytical model and the assumed actual tested structure. The obtained results for the first five natural frequencies and the difference in frequency between the analytical model and tested structure are listed in Table 4. Significant differences up to 24.9 percent in natural frequency are found due to large perturbations of mass and stiffness, and the actual modes are well correlated with the corresponding analytical modes. The proposed regularization algorithm is utilized to reduce the influence of measurement errors in cases where noise exists in the measured modal data.

The proposed approach gives the expansion results for each of the first five modes for the thin plate model, as summarized in Figs. 8–10. In the case free from noise in the modal data measurements, the proposed approach produces good expansion results with relative mode errors ranging from 0.31 to 6.2 percent. From results in Fig. 8, all expanded modes, except mode 2, are similarly sensitive to measurement noise and a 10 percent noise level does not significantly increase the relative mode errors in the expanded mode shapes. As expected, the measurement noise also affects the overall expansion performance with 9.6 percent increase in mean cumulative error and 4.9 percent increase in overall orthogonality error, when noise level increases from 0 to 10 percent, as shown in Fig. 9. The MAC diagonal values for individual expanded mode given in Fig. 10 indicate that all first five expanded modes are correctly identified and properly expanded at various levels of measurement noise, and the expanded experimental mode shapes are well correlated with the corresponding analytical modes.

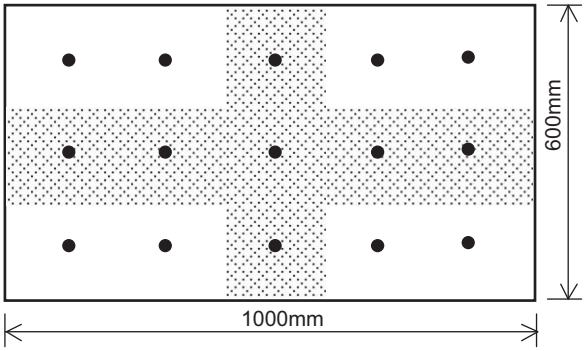

Fig. 7. Thin plate model problem with change in thickness over shaded areas and sensor locations marked with '●'.

Table 4
Ideal modes for analytical model and assumed actual thin plate structure.

Mode	Analytical frequency (Hz)	Actual frequency (Hz)	Difference in frequency (%)	MAC diagonal value
1	8.3238	9.9245	19.23	0.9990
2	30.2306	37.7570	24.90	0.9948
3	52.1533	63.5789	21.91	0.9927
4	101.4015	120.5960	18.93	0.9791
5	145.6308	171.4787	17.75	0.9066

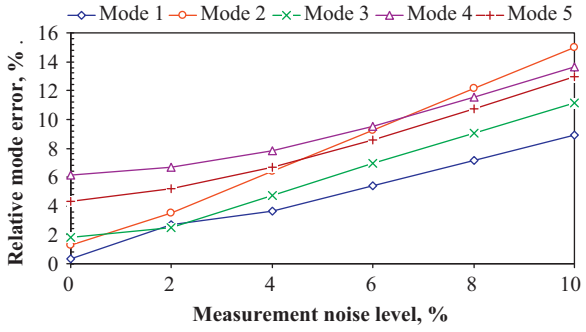

Fig. 8. Relative mode error of individual expanded mode shape as a function of noise level for thin plate structure.

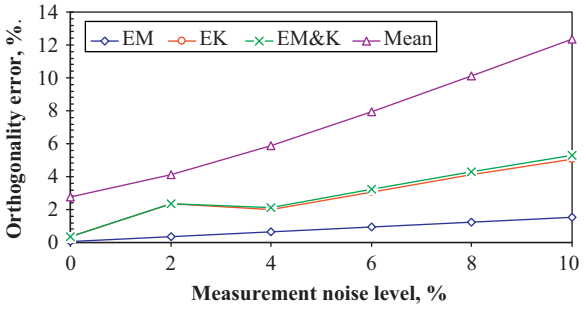

Fig. 9. Mean cumulative error and cross orthogonality errors with respect to mass and/or stiffness as a function of noise level for thin plate structure.

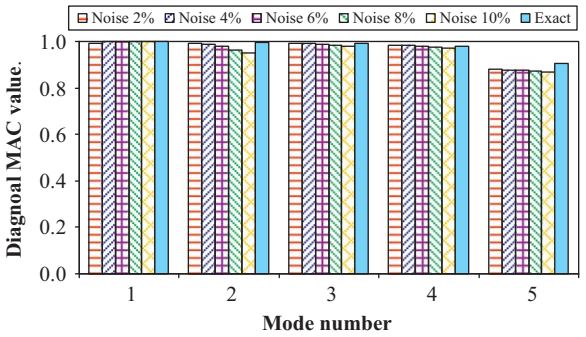

Fig. 10. MAC diagonal values for individual mode expanded by the proposed approach at various noise levels for thin plate structure.

7. Conclusions

A new approach is proposed for effectively expanding mode shapes of a complex dynamic system with limited modal data measurements, significant modelling errors and severe measurement noise. The newly developed expansion approach, based on the introduced perturbed force vector, includes the effect of discrepancies between the finite element model and the actual tested dynamic structure. The perturbed force vector containing modelling errors is adopted as the basic parameter that can be obtained from measured modal data. The unknown components of the mode shapes for the tested structure are then predicted from the obtained perturbed force vector. In the cases with noise in modal data measurements, the regularization algorithm based on the Tikhonov solution incorporating the GCV method is employed to filter out the influence of measurement uncertainties on predicting mode shape expansion. Several evaluation criteria are introduced to assess the mode shape expansion results predicted by the commonly used existing methods and the proposed approach.

Based on the verification study involving the plane frame model problem and the thin plate model problem, the following conclusions are noted: (1) The proposed approach is capable of successfully expanding mode shapes for complex dynamic systems with a large number of DOFs and produces more accurate and reliable mode shape estimates than the commonly used existing methods, in particular in the cases with significant modelling errors. (2) The knowledge of the structural parameters of the tested dynamic system is not required but included in the expansion process, and only limited information on the analytical modes is needed to produce correct mode expansion estimates. (3) Only limited number of vibration modal data measurements of the tested structure, typically <10 percent of full DOFs, could be sufficient to correctly expand the reduced measured DOF data set onto full DOF set. (4) The proposed approach performs well and produces stable and reliable results for the two different numerical examples in all simulated cases even when the modal data measurements contain a considerably high level of noise.

References

[1] D.C. Kammer, A hybrid approach to test-analysis-model development for large space structures, *Journal of Vibration and Acoustics* 113 (3) (1991) 325–332.
[2] N.A.J. Lieven, D.J. Ewins, Spatial correlation of mode shapes, the coordinate modal assurance criteria (COMAC), *Sixth International Modal Analysis Conference*, Orlando, Florida, USA, February 1988.
[3] J.E. Mottershead, M.I. Friswell, Model updating in structural dynamics: a survey, *Journal of Sound and Vibration* 167 (2) (1993) 347–375.

[4] H.P. Chen, N. Bicanic, Inverse damage prediction in structures using nonlinear dynamic perturbation theory, *Computational Mechanics* 37 (5) (2006) 455–467.
[5] P. Avitabile, A review of modal model correlation techniques, *Proceedings of NAFEM World Congress 99*, Rhode Island, USA, April 1999.
[6] M. Imregun, D. Ewins, An investigation into mode shape expansion techniques, *11th International Modal Analysis Conference*, Vol. 1, Florida, USA, February 1993, pp. 168–175.
[7] F.M. Hemez, C. Farhat, Bypassing numerical difficulties associated with updating simultaneously mass and stiffness matrices, *AIAA Journal* 33 (3) (1995) 539–546.
[8] H.P. Chen, Nonlinear perturbation theory for structural dynamic systems, *AIAA Journal* 43 (11) (2005) 2412–2421.
[9] H.P. Chen, Efficient methods for determining modal parameters of dynamic structures with large modifications, *Journal of Sound and Vibration* 298 (2006) 462–470.
[10] R. Guyan, Reduction of stiffness and mass matrices, *AIAA Journal* 3 (2) (1965) 380–387.
[11] J.C. O'Callahan, A procedure for an improved reduced system (IRS), *Seventh International Modal Analysis Conference*, Las Vegas, Nevada, USA, February 1989.
[12] M.I. Friswell, S.D. Garvey, J.E.T. Penny, Model reduction using dynamic and iterated IRS techniques, *Journal of Sound and Vibration* 186 (2) (1995) 311–323.
[13] R.L. Kidder, Reduction of structural frequency equations, *AIAA Journal* 11 (6) (1973) 892.
[14] J.C. O'Callahan, P. Avitabile, R. Riemer, System equivalent reduction expansion process, *Seventh International Modal Analysis Conference*, Las Vegas, Nevada, USA, February 1989.
[15] M. Levine-West, M. Milman, A. Kissil, Mode shape expansion techniques for prediction: experimental evaluation, *AIAA Journal* 34 (4) (1996) 821–829.
[16] A.N. Tikhonov, V.Y. Arsenin, *Solutions of Ill-Posed Problems*, Wiley, New York, 1977.
[17] G.H. Golub, M. Heath, G. Wahba, Generalized cross-validation as a method for choosing a good ridge parameter, *Technometrics* 21 (2) (1979) 215–223.